N-Terminal Aliphatic Residues Dictate the Structure, Stability, Assembly, and Small Molecule Binding of the Coiled-Coil Region of Cartilage Oligomeric Matrix Protein

ARTICLE *in* BIOCHEMISTRY · SEPTEMBER 2009

Impact Factor: 3.02 · DOI: 10.1021/bi900534r · Source: PubMed

9 AUTHORS, INCLUDING:

Wendy Hom
Stony Brook University
2 PUBLICATIONS **27** CITATIONS
SEE PROFILE

Jin Kim Montclare
New York University
48 PUBLICATIONS **499** CITATIONS
SEE PROFILE

BIOCHEMISTRY
including biophysical chemistry & molecular biology
Article

Biochemistry **2009,** *48,* 8559–8567 8559
DOI: 10.1021/bi900534r

N-Terminal Aliphatic Residues Dictate the Structure, Stability, Assembly, and Small Molecule Binding of the Coiled-Coil Region of Cartilage Oligomeric Matrix Protein†

Susheel K. Gunasekar,‡ Mukta Asnani,‡ Chandani Limbad,‡ Jennifer S. Haghpanah,‡ Wendy Hom,‡ Hanna Barra,‡ Soumya Nanda,‡ Min Lu,§ and Jin Kim Montclare*,‡,∥

‡*Department of Chemical and Biological Sciences, Polytechnic Institute of New York University, Brooklyn, New York 11201,* §*Department of Biochemistry, Weill Medical College of Cornell University, New York, New York 10021, and* ∥*Department of Biochemistry, SUNY-Downstate Medical Center, Brooklyn, New York 11203*

Received March 29, 2009; Revised Manuscript Received July 19, 2009

ABSTRACT: The coiled-coil domain of cartilage oligomeric matrix protein (COMPcc) assembles into a homopentamer that naturally recognizes the small molecule 1,25-dihydroxyvitamin D_3 (vit D). To identify the residues critical for the structure, stability, oligomerization, and binding to vit D as well as two other small molecules, all-*trans*-retinol (ATR) and curcumin (CCM), here we perform an alanine scanning mutagenesis study. Ten residues lining the hydrophobic pocket of COMPcc were mutated into alanine; of the mutated residues, the N-terminal aliphatic residues L37, L44, V47, and L51 are responsible for maintaining the structure and function. Furthermore, two polar residues, T40 and Q54, within the N-terminal region when converted into alanine improve the α-helical structure, stability, and self-assembly behavior. Helical stability, oligomerization, and binding appear to be linked in a manner in which mutations that abolish helical structure and assembly bind poorly to vit D, ATR, and CCM. These results provide not only insight into COMPcc and its functional role but also useful guidelines for the design of stable, pentameric coiled-coils capable of selectively storing and delivering various small molecules.

Cartilage oligomeric matrix protein (COMP) is a noncollagenic glycoprotein present in cartilage, tendons, ligaments, and osteoblasts (*1*−*4*). Belonging to the family of thromospondins (TSPs),[1] COMP has a pentameric boquetlike structure with a molecular mass of 524 kDa (*1*, *5*). It is composed of an N-terminal globular domain followed by an epidermal growth factor (EGF) type 2 repeat domain, a calcium binding type 3 repeat domain, and a C-terminal globular domain (*5*, *6*). The C-terminal globular domain of COMP interacts with collagen I and II and induces the formation of collagen fibrils (*7*, *8*). Mutations in COMP result in genetic disorders, including pseudoachondroplasia and multiple epiphyseal dysplasia in humans characterized by short stature and other vertebral abnormalities (*9*−*14*).

Although COMP is comprised of various domains, it is assembled into a homopentamer via an N-terminal coiled-coil domain (COMPcc). COMPcc possesses a hydrophobic pore that is 7.3 nm long with a diameter of 0.2−0.6 nm (*15*−*18*) (Figure 1). Recent structural studies reveal that the hormone 1,25-dihydroxyvitamin D_3 (vit D) can bind in the pore (*17*). This, in addition to other biochemical studies, suggests a putative role of the pentameric coiled coil in storing vit D for signaling events during morphogenesis and repair of cartilage and bone (*19*). Furthermore, COMPcc has the ability to bind hydrophobic molecules like all-*trans*-retinol (ATR), retinoic acid, elaidic acid, cyclohexane, and benzene as demonstrated by an increased thermal stability (*17*). This ability to house a variety of small molecules in the pore of the protein represents an important feature for storage and delivery.

To date, mutagenesis of the COMPcc domain has been centered on the Q54 residue since on the basis of crystallographic studies, it appears to separate the hydrophobic pore into two compartments (*17*, *20*). Mutation of Q54 into leucine resulted in higher stability (>120 °C) compared to that of COMPcc (108 °C) (*20*). A slightly different Q54I mutant bound ATR with a dissociation equilibrium constant (K_D) of 0.8 mM, exhibiting an affinity similar to that of the COMPcc (K_D = 0.6 mM) (*17*). Although these studies in addition to the structure provide insight into the significance of the single Q54 residue, there are a set of residues that line the pocket of COMPcc that may contribute to its overall structure and function that have not yet been explored.

Here we perform a single-alanine mutagenesis study to identify the ***a*** and ***d*** residues within the hydrophobic pore of COMPcc critical for the structure, stability, oligomerization, and binding to the target vit D as well as ATR and curcumin (CCM) (Figure 1). Residues within the N-terminal region extending to Q54 play a significant role in the structure and self-assembly of

†This work was supported by the Air Force Office of Scientific Research YIP (FA-9550-07-1-0060) and DURIP (FA-9550-08-1-0266) (J.K.M.), in part by the National Science Foundation MRSEC Program through Grant DMR-0820341 and GK-12 Fellows Grant 0741714 (J.S. H.), by National Institutes of Health Grant AI42382 (M.L.), by a Wechsler Award (J.K.M.), by Unilever (J.K.M.), and by the Othmer Institute for Interdisciplinary Studies (J.K.M.).

*To whom correspondence should be addressed: Department of Chemical and Biological Sciences, Polytechnic Institute of New York University, Brooklyn, NY 11201. Telephone: (718) 260-3679. Fax: (718) 260-3676. E-mail: jmontcla@poly.edu.

[1]Abbreviations: COMPcc, cartilage oligomeric matrix protein coiled coil; TSP, thromospondin; EGF, epidermal growth factor; vit D, 1,25-dihydroxyvitamin D_3; ATR, all-*trans*-retinol; CCM, curcumin; LB, Luria broth; IPTG, isopropyl thio-β-galactopyranoside; BSA, bovine serum albumin; PBS, phosphate-buffered saline; BS^3, bis-(sulfosuccinimidyl) suberate; TFA, trifluoroacetic acid; DMSO, dimethyl sulfoxide; MALDI, matrix-assisted laser desorption ionization; CD, circular dichroism; SDS−PAGE, sodium dodecyl sulfate−polyacrylamide gel electrophoresis.

Published on Web 08/14/2009

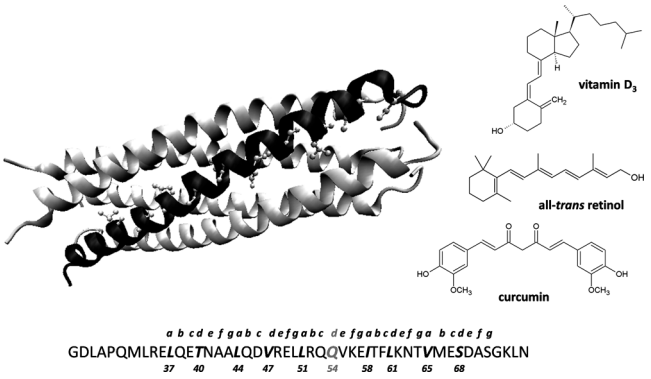

FIGURE 1: Structure and sequence of COMPcc^s in which the residues mutated into alanine are represented in bold italics, where Q54, which divides the pore into two pockets, is highlighted in gray (left). The chemical structures of the small molecules vit D, all-*trans*-retinol, and curcumin are shown (right).

COMPcc. Specifically, our studies demonstrate that the four aliphatic residues (L37, L44, V47, and L51) are necessary for maintaining helical content, stability, pentamer structure, and small molecule recognition. By contrast, the two polar residues (T40 and Q54) when mutated into alanine facilitate α-helix formation, thermal stability, and oligomerization state, while maintaining vit D and ATR binding. These results bear interesting implications on what dictates COMPcc oligomerization and provide guidelines for the design of highly helical and stable pentamers capable of binding specific small molecules (*21*−*23*).

EXPERIMENTAL PROCEDURES

Materials. The oligonucleotides were purchased from Sigma. The *pfu* Ultra enzyme for performing the site-directed mutagenesis was from Stratagene. *Dpn*I restriction enzyme was purchased from Roche Diagnostics. Sodium phosphate (monobasic and dibasic), Trizma base, Ni-NTA resins, acetonitrile, trifluoroacetic acid (TFA), dimethyl sulfoxide (DMSO), and α-cyano-4-hydrocinnamic acid were from Sigma-Aldrich. Isopropyl β-D-thiogalactopyranoside (IPTG), ampicillin, tryptone, sodium chloride, and urea were purchased from Fisher. Methanol, yeast extract, all-*trans*-retinol (ATR), and curcumin (CCM) were from Acros. 1,25-Dihydroxyvitamin D_3 (vit D) was purchased from Alfa Aesar. The MicroBCA kit was from Pierce, and bis-(sulfosuccinimidyl) suberate (BS^3) was purchased from Thermo Scientific.

Site-Directed Mutagenesis. The COMPcc gene in the pQE9 vector (gift from K. Zhang) was used as the template for site-directed mutagenesis. Residues L37, T40, L44, V47, L51, Q54, I58, L61, V65, and S68 at the ***a*** and ***d*** positions were mutated to alanine using the following primers and their complements: L37A, 5′-GCTGCGTGAAGCGCAGGAAACCAACGCGG-3′; T40A, 5′-GAACTGCAGGAAGCGAACGCGGCGCTGC-3′; L44A, 5′-CCAACGCGGCGGCGCAGGACGTCGTG-3′; V47A, 5′-GCGCTGCAGGACGCGCGTGAACTGCTGC-3′; L51A, 5′-GGACGTTCGTGAACTGGCGCGTCAGCAGG-3′; Q54A, 5′-CGTGAACTGCTGCGTCAGGCGGTTAAAGA-AATCACC-3′; I58A, 5′-CTGCGTCAGCAGGTTAAAGA-AGCGACCTTCCTGAAAAACACC-3′; L61A, 5′-GAA-ATCACCTTCGCGAAAAACACCGTTATGGAATGTGA-CG-3′; V65A, 5′-CTGAAAAACACCGCGATGGAATGT-GACGCGTGTGG-3′; S68A, 5′-CTGAAAAACACCGTTA-TGGAAGCGGACGCGTGTGGTAAGC-3′. The mutations were confirmed by DNA sequencing.

Expression and Purification. *Escherichia coli* strain XL1 Blue was used as the host strain for the mutants. Starter cultures were grown at 37 °C and 250 rpm in Luria broth bearing 1 mM ampicillin (LB-amp). An approximately 1:500 dilution of the starter cultures was used for large-scale expression in LB-amp and allowed growth at 37 °C and 250 rpm. When an optical density of 1.0 at 600 nm had been reached, proteins were induced by addition of 1 mM isopropyl β-D-thiogalactopyranoside (IPTG) and allowed to incubate at 37 °C and 250 rpm for 3 h. Cells were harvested and stored at −80 °C. The cell pellet was thawed and resuspended in equilibration buffer [0.1 M sodium phosphate monobasic, 10 mM Trizma base, and 8 M urea (pH 8.0)]. Purification was conducted under denaturing conditions using Ni-NTA affinity resin, and the proteins were eluted at lower pH values of 5.47, 5.12, and 4.44. The denatured protein was refolded by dialysis containing 6 and 4 M urea in 100 mM phosphate buffer (pH 8.0) each for 3 h at 4 °C. The last step of dialysis is repeated three times containing 100 mM phosphate buffer (pH 8.0) each for 3 h at 4 °C. The purified protein concentration was estimated by the MicroBCA kit using bovine serum abumin (BSA) as a standard. To confirm the molecular masses of the proteins, matrix-assisted laser desorption ionization (MALDI) mass spectrometry was performed using an Omniflex Bruker Daltonics Instrument and analyzed with XMassOmniflex Analyzer. The calculated molecular masses of all the proteins were in the range of the expected molecular mass of 6.9 kDa (Table S1 of the Supporting Information).

Circular Dichroism. Circular dichroism (CD) spectroscopy was conducted on a Jasco J-815 CD spectrometer in which all proteins were at a concentration of 10 μM. The wavelength spectrum was measured over a range from 190 to 250 nm with a step size of 1 nm. Temperature scans of each protein were performed over a range of 25−85 °C with a temperature step of 0.1 °C/min. This temperature range was selected on the basis of previous COMPcc CD work from others (*17*) and from our lab (data not shown). The starting temperature of 25 °C was chosen since the wavelength scans at this temperature revealed stable helical structures for COMPcc^s (vida infra). All scans were made in duplicate. The ellipticity value (Θ) was converted to mean molar residue ellipticity (MRE) using the following conversion (*24*)

$$\Theta_{MRE} = \Theta/(10cpl) \quad (1)$$

where c is the molar concentration of the protein, p is the path length in centimeters, and l is the number of amino acids in the protein.

The fraction helicity (f) was calculated using the expression (*25*)

$$f = 100[(\Theta)_{222}/(\Theta_{max})_{222}] \quad (2)$$

where $(\Theta_{max})_{222} = -40000[1 - (2.5/n)]$ ($n = 61$).

The fraction folded (F) was estimated using the conversion (*26*)

$$F = (\Theta_A - \Theta_U)/(\Theta_N - \Theta_U) \quad (3)$$

where Θ_A is the observed MRE, Θ_U is the MRE value at the unfolded state, and Θ_N is the MRE at the native state. The melting temperature (T_m) of each protein was calculated by plotting the first derivative of fraction folded versus the temperature.

The thermodynamic parameters were estimated from the thermal denaturation curves assuming a two-state model for those proteins that exhibited a reversible melting curve (*27*). The

self-association and dissociation of COMPcc (pentamer) follow the equilibrium reaction (*28*, *29*)

$$5U \leftrightarrow N_5 \quad (4)$$

The equilibrium constant (k) for reaction 4 is expressed in terms of fraction folded (F) by

$$k = F/5C_T{}^4(1-F)^5 \quad (5)$$

where C_T = [U] + 5[N] represents the total peptide concentration. The Gibbs free energy of folding ($\Delta G°$) is given by

$$\Delta G° = -RT \ln k = \Delta H° - T\Delta S° \quad (6)$$

where $\Delta H°$ and $\Delta S°$ signify the standard enthalpy and entropy change, respectively. The van't Hoff enthalpy ($\Delta H°$) was calculated at the thermal midpoint of transition (T_m) of the melting curve using the following equation

$$\Delta H° = ART_m{}^2(dF/dT)_{T=T_m} \quad (7)$$

where A = 12 for a pentamer. Under equilibrium, $\Delta S° = (\Delta H°)/T_m$ which allows for the calculation of the change in entropy. The $\Delta G°$ at 25 °C (298 K) was calculated using eq 6.

When $T = T_m$ and $F = 0.5$, it follows from eq 5 that

$$T_m = \Delta H°/\Delta S° + R\ln(0.31C_T{}^4) \quad (8)$$

Solving for $\Delta S°$ from eq 8 and substituting in eq 6 result in the following expression

$$k = \exp[\Delta H°/R(1/T_m - 1/T) - \ln(0.31C_T{}^4)] \quad (9)$$

The $\Delta H°$ was calculated using eq 7, which was then used to recalculate the equilibrium constant (k) using eq 9. The k value obtained was used to recalculate F from eq 5. The resulting values of F were plotted and employed to determine the $\Delta H°$ value.

CD studies in the presence of vit D were conducted by allowing the protein to bind vit D overnight at 4 °C. The protein was centrifuged to remove any excess vit D, and wavelength and thermal scans were conducted for most of the samples. Variants Q54A, L61A, V65A, and S68A were heated to their respective T_m values, and vit D was added to facilitate binding. They were gradually cooled to room temperature and allowed to bind overnight at 4 °C.

Chemical Cross-Linking. The oligomerization states of the proteins were determined by chemical cross-linking using bis-(sulfosuccinimidyl) suberate (BS^3) ester with a spacer arm of 11.4 Å (*30*). Proteins were incubated with 1.5 mM BS^3 in 100 mM phosphate buffer (pH. 8.0) for 1 h at room temperature. The reaction was quenched via addition of 25 mM Trizma base. Sodium dodecyl sulfate (12%)−polyacrylamide gel electrophoresis (SDS−PAGE) was used to identify the cross-linked states of the proteins. Similarly, vit D was bound overnight to the proteins at 4 °C, and cross-linking studies were conducted.

Sedimentation Equilibrium Analysis. Analytical ultracentrifugation measurements were taken on a Beckman XL-A (Beckman Coulter) analytical ultracentrifuge equipped with an An-60 Ti rotor (Beckman Coulter) at 20 °C. Protein samples were dialyzed overnight against PBS [100 mM sodium phosphate and 100 mM NaCl (pH 8.0)], loaded at initial concentrations of 50 and 200 μM, and analyzed at rotor speeds of 17000 and 20000 rpm. Data were acquired at two wavelengths per rotor speed setting and processed simultaneously with a nonlinear least-squares fitting routine (*31*). The solvent density and protein partial specific volume were calculated according to solvent and protein composition, respectively (*32*).

Fluorescence. Fluorescence measurements of the protein·ATR and protein·CCM complexes were performed with 9.5 μM protein and 40 μM ATR or 50 μM CCM in 100 mM phosphate buffer (pH 8.0) with 0.4% DMSO and 0.5% methanol, respectively. After the samples had been incubated for 30 min at room temperature, fluorescence was measured using a SpectraMax Plus M2 instrument with an excitation wavelength of 330 nm and an emission wavelength from 360 to 600 nm in the case of ATR (*17*). For CCM binding, fluorescence was monitored with an excitation wavelength of 420 nm and an emission wavelength from 450 to 600 nm (*33*, *34*). For both ATR and CCM, the maximal peak was identified from the emission spectrum. Most proteins demonstrated an emission maximum near 460 and 490 nm for ATR and CCM, respectively. For CCM binding, two variants, I58A and L61A, possessed maxima near 460 nm. A time course study was conducted to identify the optimal equilibration time for both small molecules. Controls of buffer, protein, ATR, and CCM alone did not demonstrate an increase in fluorescence. All fluorescence measurements were taken in triplicate. Error bars denote the standard deviation.

RESULTS

COMPcc^s and Alanine Variants. The original COMPcc sequence bears two cysteines (C68 and C71) near the C-terminus that form disulfide bridges which stabilize the pentamer (*17*). To investigate the behavior of the proteins without the complication of oxidation, the cysteines were mutated into serines and used as our template (COMPcc^s) for single-alanine mutagenesis (Figure 1). The 10 residues in the ***a*** and ***d*** positions lining the pore of COMPcc^s were individually mutated to alanine via site-directed mutagenesis. Each alanine variant in addition to the COMPcc^s was characterized for structure, stability, and oligomerization state. Binding of the variants to the hydrophobic small molecules vit D, ATR, and CCM was also assessed.

Impact of Variants on α-Helicity. Far-UV circular dichroism (CD) was employed to determine the secondary structure of COMPcc^s and variants at room temperature (*35*). A wavelength scan of COMPcc^s demonstrated double minima at 208 and 222 nm indicative of an α-helix with a calculated fractional helicity of 70.1% as previously reported (*20*) (Figure 2a and Table 1). This confirmed that mutation of the cysteines to serines within the COMPcc sequence did not significantly alter the structure of the protein. Variants L37A, L44A, V47A, L51A, and I58A exhibited a substantial loss of α-helical structure (Figure 2a and Table 1). Each of these variants expressed a fractional helicity with less than 50% and a $\Theta_{222}/\Theta_{208}$ of < 1, indicating that these residues are critical for the maintenance of α-helix. Variants L61A, V65A, and S68A exhibited a modest decrease or no change in helical content (Figure 2a and Table 1). These variants possessed a 58−69% fractional helicity and retained a $\Theta_{222}/\Theta_{208}$ of ≥ 1. Finally, the two variants T40A and Q54A illustrated an increase in α-helicity as demonstrated by the $> 80\%$ fractional helicity values and the $\Theta_{222}/\Theta_{208}$ of > 1.

Of the total residues that line the N-terminal pocket divided by Q54, all the aliphatic residues (L37, L44, V47, and L51) appear to play a significant role in maintaining the helix (Figure 1). Residue I58 is the only residue located within the second C-terminal pocket that yielded a significant loss in helical content when mutated to alanine. The remaining residues (L61, V65, and S68)

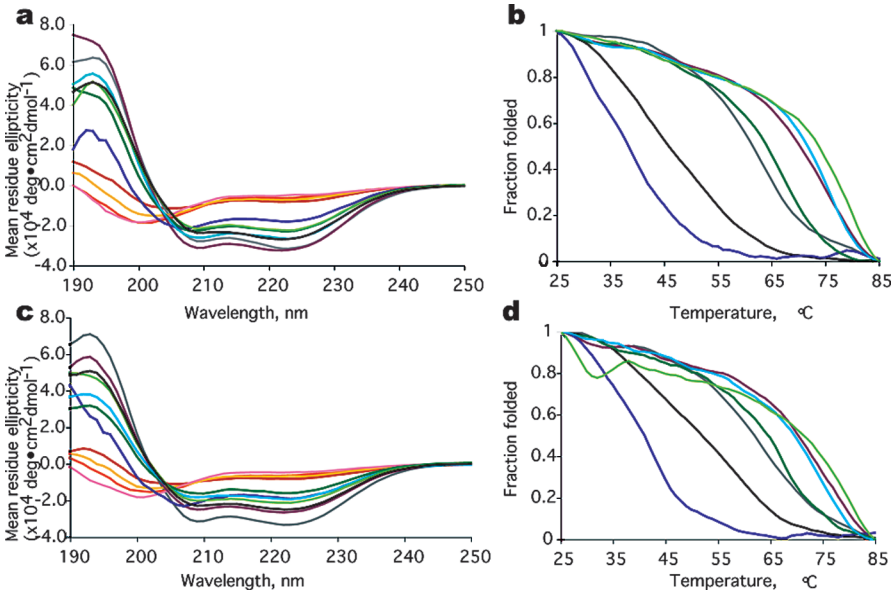

FIGURE 2: CD spectra of COMPcc^s and single-alanine variants in the absence (a and b) and presence (c and d) of vit D. (a and c) Wavelength scans at room temperature (25 °C) and (b and d) temperature scans at 222 nm of COMPcc^s (black), L37A (red), T40A (gray), L44A (orange), V47A (yellow), L51A (pink), Q54A (purple), I58A (blue), L61A (green), V65A (light blue), and S68A (light green). All scans represent an average of two trials.

Table 1: Summary of Structure and Stability Comparison from Circular Dichroism Studies

	without 1,25-dihydroxyvitamin D_3					with 1,25-dihydroxyvitamin D_3					
protein	$-\Theta_{208}$ (deg cm^2 dmol^{-1})	$-\Theta_{222}$ (deg cm^2 dmol^{-1})	$\Theta_{222}/\Theta_{208}$	fraction helicity (%)	T_m (°C)	$-\Theta_{208}$ (deg cm^2 dmol^{-1})	$-\Theta_{222}$ (deg cm^2 dmol^{-1})	$\Theta_{222}/\Theta_{208}$	fraction helicity (%)	T_m (°C)	ΔT_m (°C)
COMPcc^s	22727.3	26928	1.18	70.1	41	22178	25045.3	1.12	65.2	45	4
L37A	10806.3	8333.75	0.77	21.7	–	10625	8196.28	0.77	21.3	–	–
T40A	26648.4	31579.8	1.18	82.2	62	30612	33385.1	1.09	86.9	63	1
L44A	12814.5	6397.98	0.49	16.6	–	11103.2	6521.12	0.58	16.9	–	–
V47A	12131.3	7377.34	0.6	19.2	–	10915.1	6861.03	0.62	17.8	–	–
L51A	10636.6	5139.54	0.48	13.3	–	10424.3	4782.02	0.45	12.4	–	–
Q54A	30283.6	32498.7	1.07	84.6	74	24492.1	26604.3	1.08	69.2	77	3
I58A	21299.3	18118.1	0.85	47.1	38	22177.5	18588	0.83	48.4	41	3
L61A	22773.3	22985.7	1.0	59.8	67	15916.2	16169.2	1.01	42.1	67	0
V65A	25745.7	26518.2	1.03	69	76	18181.2	19247.2	1.05	50.1	75	−1
S68A	20896	22396.6	1.07	58.3	80	19754.8	21285.2	1.07	55.4	81	1

within the C-terminal pocket bear modest implications on the α-helix. The two polar residues, T40 and Q54, improve the helical content when mutated to alanines in the N-terminal pocket. Together, this suggests that the residues within the N-terminal pocket are important in establishing and maintaining the helical structure, while the C-terminal residues do not substantially influence the α-helix.

Impact of Variants on Thermostability. Temperature scans at 222 nm were performed to determine the thermostabilities of all the proteins under identical concentrations of 10 μM (*36*). The COMPcc^s presented a cooperative thermal transition temperature (T_m) of 41 °C, similar to previously reported values (*17*). Of the six variants that produced a discernible melting curve, five demonstrated a significant increase in thermostability relative to that of COMPcc^s (Figure 2b and Table 1). Variant S68A displayed a 39 °C enhancement in T_m, the largest increase observed for any variant. This was followed by the values of V65A and Q54A, which showed improvements of 35 and 33 °C, respectively, while variants L61A and T40A presented increases of 26 and 21 °C relative to that of COMPcc^s, respectively. By contrast, variant I58A displayed a 3 °C decrease in T_m, when compared to that of COMPcc^s.

The reversibility and monophasic behavior of the melts enable us to assume a two-state mechanism of unfolding (*27*−*29*). As a result, we can calculate the thermodynamic parameters of the aforementioned variants and COMPcc^s based on the fraction folded (*28*, *29*, *37*). The stability of COMPcc^s arises from a strong enthalpic component with a van't Hoff enthalpy ($\Delta H°$) of −85.2 kcal/mol (Table 2). This leads to a calculated Gibbs free energy ($\Delta G°$) of −4.3 kcal/mol within the range of the other coiled-coil systems, including human cartilage oligomeric matrix protein (*29*, *30*), tetramers (*30*), and dimers (*38*). In general, for the T40A and Q54A variants that exhibited enhanced helical content and stability, increases in free energy of 8.4 and 13.4 kcal/mol are observed relative to that of COMPcc^s, respectively (Table 2). The remaining C-terminal residues (L61, V65, and S68) demonstrated 11.3, 19.4, and 22.7 kcal/mol increases in stability, respectively, compared to that of COMPcc^s when mutated to alanine (Table 2). By contrast, I58A revealed a minimal change in stability relative to that of COMPcc^s of 0.2 kcal/mol (Table 2).

The majority of the residues that impact the thermostability are located within the C-terminal pocket starting from the division point of Q54 (Figure 1). C-Terminal residues L61,

Table 2: Summary of the Calculated Thermodynamic Parameters

	without vitamin D			with vitamin D		
protein	$\Delta H^{\circ a}$ (kcal/mol)	$\Delta S^{\circ b}$ (kcal mol^{-1} K^{-1})	$\Delta G^{\circ c}$ (kcal/mol)	$\Delta H^{\circ a}$ (kcal/mol)	$\Delta S^{\circ b}$ (kcal mol^{-1} K^{-1})	$\Delta G^{\circ c}$ (kcal/mol)
COMPcc^s	−85.2	−0.27	−4.3	−64.7	−0.20	−4.0
T40A	−115.3	−0.34	−12.7	−104.1	−0.30	−11.7
Q54A	−125.9	−0.36	−17.7	−129.6	−0.37	−19.2
I58A	−109.98	−0.35	−4.5	−133.6	−0.42	−6.7
L61A	−127.7	−0.37	−15.6	−146.8	−0.43	−18.1
V65A	−162.4	−0.46	−23.7	−130.2	−0.37	−18.7
S68A	−173.3	−0.49	−27	−144.9	−0.40	−22.9

[a] van't Hoff enthalpy calculated as described in Experimental Procedures. [b] At equilibrium, $\Delta G^\circ = 0$. Hence, the change in entropy (ΔS°) = $\Delta H^\circ / T_m$. [c] Free energy of folding at 25 °C calculated by the expression $\Delta G^\circ = \Delta H^\circ - T\Delta S^\circ$.

V65, and S68 stabilize the protein when mutated to alanine, while alanine at position 58 does not significantly impact stability. Although most of residues that influence stability are localized on the C-terminal end, T40 and Q54 within the first pocket also affect the thermostability when converted to alanine. The enhancement in stability observed by these two variants appears to be linked to the improved helical content described above.

Impact of Variants on Oligomerization State. To determine the oligomerization states of COMPcc^s and variants, cross-linking studies were performed using bis(sulfosuccinimidyl) suberate (BS^3) at the same concentrations used for CD and analyzed via SDS−PAGE (*30*). The COMPcc^s demonstrated the presence of five equally intense bands indicating the presence of pentamers, in addition to tetra-, tri-, di-, and monomers (Figure 3). In contrast, variants L37A, L44A, V47A, and L51A exhibited predominantly monomer bands. Both L44A and L51A showed evidence for dimer in addition to monomer. V47A displayed the existence of di-, tri-, and tetramers, while L37A demonstrated the presence of di-, tri-, tetra-, and pentamers with less intensity than the monomer band. Variants T40A, Q54A, I58A, L61A, V65A, and S68A illustrated an enhanced oligomerization in which the monomer band disappeared, while retaining the di-, tri-, tetra-, and pentamer bands (Figure 3). In general, residues L37, L44, V47, and L51 are important for maintaining the oligomeric state of the protein and are positioned in the N-terminal pocket region since mutation to alanine abolishes the presence of the pentamer bands.

Furthermore, sedimentation equilibrium experiments indicate that the apparent molecular masses of COMPcc^s and the T40A, Q54A, I58A, L61A, V65A, and S68A variants were within 10% of those calculated for a pentamer, with no systematic deviation of the residuals (Figure 4 and Table 3). Hence, residues T40, Q54, I58, L61, V65, and S68 do not appear to be critical for pentamerization. In fact, mutation to alanine facilitates oligomerization. These residues are mostly distributed at the C-terminal end with the exception of two polar residues, T40 and Q54, that reside in the N-terminal region.

Influence of 1,25-dihydroxyvitamin D$_3$. One of the key features of COMPcc is its ability to bind vit D as demonstrated by structural and biochemical studies (*17*). vit D is an important hormone involved in promoting cellular differentiation and proliferation in terms of cartilage and bone tissue in addition to the maintenance of calcium and phosphate homeostasis (*39*, *40*). To investigate the impact of the presence of vit D, we performed CD and cross-linking studies after incubating COMPcc^s and variants with the small molecule.

The proteins before and after binding vit D were compared to evaluate whether there is any effect of vit D on helicity. Variants L37A, L44A, V47A, L51A, I58A, L61A, V65A, and S68A exhibiting large and modest losses in α-helical content revealed similar decreases, while variants T40A and Q54A demonstrating enhanced helicity maintained an increase with respect to that of COMPcc^s in the presence of vit D (Figure 2c and Table 1). Nearly all the variants, including COMPcc^s, exhibited a slight loss of helical content upon incubation with vit D relative to the unbound proteins, except T40A, L44A, and I58A.

As described for the variants in the absence of vit D, similar increases and decreases in T_m were observed relative to that of COMPcc^s (Figure 2d and Table 1). Variants Q54A, V65A, S68A, L61A, and T40A presented increases in T_m ranging from 36 to 18 °C, while I58A showed a decrease in T_m of 4 °C when compared to that of COMPcc^s. Previously, COMPcc binding to vit D was detected by a shift in the T_m (*17*). COMPcc^s demonstrated an increase in the T_m of 4 °C upon incubation with vit D, affirming earlier data (*17*) (Figure 2d and Table 1). Variants I58A and Q54A each exhibited a 3 °C increase, followed by S68A which revealed a 1 °C enhancement. However, variant L61A did not affect the T_m, while V65A illustrated a decrease in T_m by 1 °C (Figure 2d and Table 1). Variants L37A, L44A, V47A, and L51A were unable to bind vit D because of their inability to form α-helices.

To study the impact of vit D on oligomerization, cross-linking studies were performed after incubation with vit D. A similar trend was observed in which L37A, L44A, V47A, and L61A demonstrated mostly monomers or a lack of pentamer formation, while the remaining T40A, Q54A, I58A, L61A, V65A, and S68A variants exhibited strong pentamer bands (Figure S1 of the Supporting Information).

Binding to all-trans-Retinol and Curcumin. Guo and coworkers demonstrated that COMPcc is capable of binding hydrophobic small molecules such as ATR in addition to the target vit D (*17*). ATR, also known as vitamin A, is critical for organ tissue and limb growth in both embryonic cells and adult tissue (*41*, *42*). Because of its unique fluorescence behavior, the binding of ATR to COMPcc can be readily monitored spectrophotometrically (*17*). To explore the effect of the mutations on ATR recognition, we investigated binding via fluorescence.

Variants L37A, L44A, V47A, L51A, I58A, and L61A demonstrated dramatic losses in their levels of binding, indicating that these residues may be critical for ATR recognition (Figure 5). The N-terminal residues L37, L44, V47, and L51 responsible for the maintenance of helical content and oligomerization state bound poorly to ATR when substituted with alanine. By contrast, the Q54A variant that previously illustrated enhanced helical content and oligomerization revealed an increase in fluorescence, indicative of improved binding. Interestingly, S68A previously shown to display modest effects on the

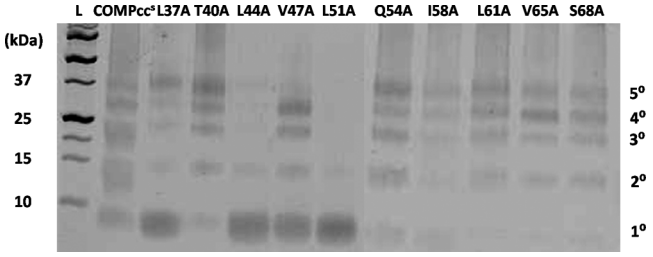

FIGURE 3: SDS−PAGE of cross-linking of variants by bis(sulfosuccinimidyl) suberate (BS^3). Lane L contained protein markers. The cross-linked samples were subjected to 12% SDS−PAGE to determine the oligomerization state of the variants. The molecular masses are indicated at the left, and the monomer (1°), dimer (2°), trimer (3°), tetramer (4°), and pentamer (5°) populations are indicated at the right.

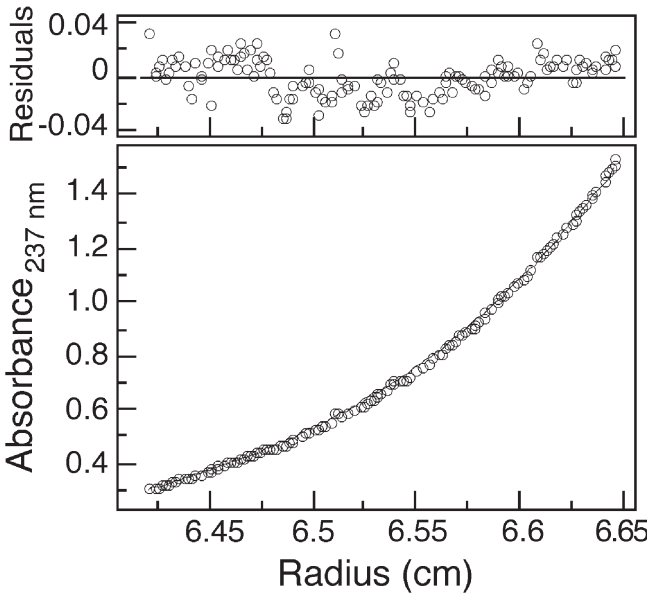

FIGURE 4: Representative equilibrium sedimentation data (17000 rpm) of I58A (~200 μM) in PBS at 20 °C. The data fit closely to a pentameric complex. The deviation in the data from the linear fit for a pentameric model is plotted (top).

Table 3: Sedimentation Equilibrium Data of COMPcc^s and Variants

protein	$M_{obs}/M_{monomer}$[a]	protein	$M_{obs}/M_{monomer}$[a]
COMPcc^s	4.9	L61A	4.9
T40A	4.8	V65A	5.0
Q54A	4.8	S68A	5.1
I58A	5.0		

[a] $M_{obs}/M_{monomer}$ is the apparent molecular mass determined from sedimentation equilibrium data divided by the expected mass of a monomer.

coiled-coil structure and self-assembly also bound slightly better to ATR.

Because of the predominant hydrophobicity of the COMPcc pore, it has been suggested that the protein may potentially bind other retinoids and hydrophobic compounds (*17*). Curcumin (CCM) is a polyphenol isolated from turmeric bearing unique pharmacological activity, including anticarcinogenic (*43*, *44*), antioxidant (*45*), and antihypertrophy (*46*, *47*) properties. Like ATR, it can be monitored for binding to the variants because of its fluorescence behavior (*33*, *34*). We sought to investigate the

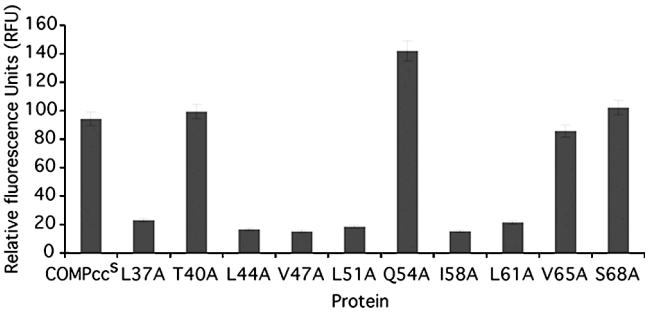

FIGURE 5: ATR fluorescence binding studies of COMPcc^s and variants. Protein·ATR complexes were excited at 330 nm, and emission maxima for each mutant were obtained. Plots represent an average of three trials in which error bars denote the standard deviation.

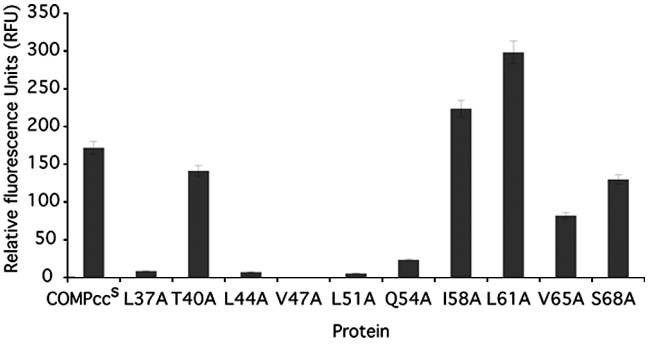

FIGURE 6: CCM fluorescence binding studies of COMPcc^s and variants. Protein·CCM complexes were excited at 420 nm, and emission maxima for each mutant were obtained. Plots represent an average of three trials in which error bars denote the standard deviation.

binding of the variants to CCM in part because of its structural difference from the retinoids and seco steroid vit D.

Variants L37A, L44A, V47A, L51A, and Q54A demonstrated significant reductions in their levels of binding (Figure 6). The four residues (L37, L44, V47, and L51) positioned in the N-terminal pocket that were previously noted to be essential for helicity and oligomerization also bound CCM poorly when substituted with alanine, which is similar to the ATR studies. Notably, I58A and L61A revealed an increase in fluorescence relative to that of COMPcc^s (Figure 6). Comparison of ATR and CCM binding studies reveals a consistency in the binding abilities of the variants for both substrates; however, variants Q54A, I58A, and L61A demonstrate a clear preference for either ATR or CCM. These results suggest that the residues that line the pocket play an important role in selectively binding various hydrophobic small molecules.

DISCUSSION

Coiled-coil proteins have been extensively studied because of their significance in biological systems (*48*−*54*). They are distinguished by heptad repeats (*abcdefg*) in which the residues in the ***a*** and ***d*** positions play a significant role in its overall structure (*48*). COMPcc represents a coiled coil that assembles into a pentamer of parallel α-helices. Of the 10 residues in the ***a*** and ***d*** positions of COMPcc^s, L37, L44, V47, and L51 are responsible for maintaining the structure (Figure 1). These aliphatic residues when mutated to alanine result in a loss of helical structure, stability, and oligomerization state. By contrast,

polar residues T40 and Q54 within the N-terminal region when converted to alanine improve the α-helical structure, stability, and self-assembly behavior.

Interplay of Helicity, Stability, and Oligomerization. Residues L37, L44, V47, and L51 that exhibited a substantial loss of helicity when substituted with alanine were not sufficiently stable to determine melts, while I58A which showed a modest loss of α-helical structure demonstrated a loss in T_m (Table 1). These results suggest that the residues critical for maintaining helical content are important for preserving stability. Moreoever, residues L37, L44, V47, and L51 that no longer displayed helical structure and discernible stability when mutated to alanine revealed predominantly monomeric states (Figures 2 and 3). These data are consistent with the previous work by Miura and co-workers in which alanine mutation of synthetic peptides that led to an abolishment in α-helix also prevented the formation of fibrous assembly (*55*).

The residues important for structure, stability, and pentamer formation are located in the N-terminal pocket. On the basis of the heptad pattern, L37, L44, and L51 occupy the ***a*** position while V47 occupies the ***d*** position (Figure 1). Thus, the stability of the pentameric assembly is largely mediated by the interactions between three leucines from one helix with a valine from the adjacent helix. Another pentameric coiled-coil, phospholamban, has been demonstrated to be governed by the packing interactions among three N-terminal leucines, L37, L44, and L51, in the ***a*** position with two isoleucines, I40 and I47, in the ***d*** position from a neighboring helix (*56*, *57*). This suggests that an N-terminal repeat of three leucines in the ***a*** site along with a valine or set of isoleucines in the ***d*** site of the adjacent helix is indispensible for the formation of pentamers.

The two polar residues, T40 and Q54, that improved the α-helical content when mutated to alanine also demonstrated a substantial increase in T_m (Table 1). Alanine substitution of either residue in this N-terminal region resulted in pentamer formation and enhanced oligomerization (Figures 3 and 4 and Table 3). In this case, increased helicity and stability facilitate oligomer formation.

The remainder of residues L61, V65, and S68 located in the C-terminal region when substituted with alanine yielded a modest loss of helical content (within 15%), while exhibiting an enhanced stability (Table 1). Interestingly, alanine substitution of these residues maintains pentamer formation and improves the oligomerization state where the monomer population essentially disappears (Figures 3 and 4 and Table 3). Here, the C-terminal residues maintain the link between stability and oligomerization as long as a threshold level of α-helical structure is maintained.

Influence of vit D on Helicity, Stability, and Oligomerization. No significant change in helical content, stability, or oligomerization was observed in the presence of vit D for the COMPcc^s and alanine variants relative to the unincubated proteins (Table 1). The major discernible differences can be identified from shifts in the T_m. Variants T40A, Q54A, I58A, L61A ,and S68A in addition to COMPcc^s exhibited an increase or no change in their T_m values, indicating binding of vit D. These five span both pockets with a majority concentrated in the C-terminus and do not play a significant role in vit D recognition. Variant V65A exhibits a decrease in T_m, suggesting that it may be important for vit D binding. However, residues L37, L44, V47, and L51 represent the most crucial in vit D recognition as absolutely no binding can even occur because of the inability to oligomerize as described above.

Variants That Exhibit a Specific Preference for vit D, ATR, or CCM. From the vit D, ATR, and CCM studies, variants Q54A, I58A, and L61A demonstrated selective binding. Variant Q54A exhibited an enhanced affinity for ATR while illustrating poor binding to CCM and vit D (Figures 2d, 5, and 6). Remarkably, two variants, I58A an L61A, bound specifically to CCM, while weakly binding ATR and vit D (Figures 2d, 5, and 6). Thus, by altering the sequence within the binding pocket, one may be able to control the specificity for small molecule binding.

Structural Data Add Molecular Detail to Interactions with Small Molecules. On the basis of the structural analysis of COMPcc·vit D (*19*) and COMPcc·ATR (*17*) complexes, Q54 separated the core into two distinct cavities. The vit D binds both pockets, while ATR is occupied exclusively in the N-terminal cavity. Both small molecules are poised between the T40 and Q54 residues. T40 recognizes the dimethyl group of vit D (*19*) and the β-ionine ring of ATR (*17*). Q54 mediates a H-bond contact to the hydroxyl group of ATR while providing separation within the cavity for both ATR and vit D (*17*, *20*). While both residues appear to make contacts with both small molecules, they are not needed as demonstrated by previous biochemical studies and our mutagenesis data (*17*, *20*).

Both cocrystal structures reveal that residues L44, V47, and L51 lining the N-terminal cavity can accommodate vit D and ATR even though both small molecules differ structurally (*17*, *20*). For the COMPcc·vit D complex, V47 is able to accommodate the seco B ring system, imposing a planar 6-s-*trans* conformation of vit D, while residue L44 interacts with the methyl C18 atom of the C ring on the β face (*19*). In the case of the COMPcc·ATR complex, L44 contacts the C16, C17, and C18 methyl groups of the β-ionine of ATR, while the cavities between L44−V47 and V47−L51 interact with the C19 and C20 methyl moieties of the isoprene group (*17*). Our data confirm that mutation of any of these three residues results in poor binding to either compound. Moreover, these residues are also important for CCM binding, indicating their significance for small molecule recognition.

CONCLUSION

Here we show that the helicity, stability, oligomerization, and small molecule binding of COMPcc are predominantly controlled in positive and negative ways by the residues within the N-terminal region. Four N-terminal aliphatic residues are necessary for maintaining the structure and self-assembly, while the two polar residues are dispensable. Alanine substitution of the two polar residues renders variants that are more helical and thermostable and facilitate pentamer formation. These findings have interesting implications on how COMPcc is able to maintain its structure and function. Moreover, the lessons learned from these studies can aid in the design of exceptionally stable artificial oligomeric coiled coils (*21*−*23*, *58*) capable of binding various small molecules with high selectivity (*17*). Future studies employing COMPcc variants in the context of artificial peptides or proteins for specific binding and delivery of small molecules as potential biomaterials are underway (*50*, *59*−*63*).

ACKNOWLEDGMENT

We thank Neville Kallenbach and anonymous reviewers for assistance and critical insight into the experiments and manuscript.

SUPPORTING INFORMATION AVAILABLE

The MALDI data to confirm the molecular weights of the proteins and the cross-linking studies of the proteins in the presence of vit D. This material is available free of charge via the Internet at "http://pubs.acs.org".

REFERENCES

1. Hedbom, E., Antonsson, P., Hjerpe, A., Aeschlimann, D., Paulsson, M., Rosapimentel, E., Sommarin, Y., Wendel, M., Oldberg, A., and Heinegard, D. (1992) Cartilage Matrix Proteins: An Acidic Oligomeric Protein (Comp) Detected Only in Cartilage. *J. Biol. Chem. 267*, 6132–6136.
2. Dicesare, P., Hauser, N., Lehman, D., Pasumarti, S., and Paulsson, M. (1994) Cartilage Oligomeric Matrix Protein (Comp) Is an Abundant Component of Tendon. *FEBS Lett. 354*, 237–240.
3. Muller, G., Michele, A., and Altenburg, E. (1998) COMP (cartilage oligomeric matrix protein) is synthesized in ligament tendon, meniscus and articular cartilage. *Connect. Tissue Res. 39*, 233–244.
4. Di Cesare, P. E., Fang, C., Leslie, M. P., Tulli, H., Perris, R., and Carlson, C. S. (2000) Expression of cartilage oligomeric matrix protein (COMP) by embryonic and adult osteoblasts. *J. Orthop. Res. 18*, 713–720.
5. Oldberg, A., Antonsson, P., Lindblom, K., and Heinegard, D. (1992) Comp (Cartilage Oligomeric Matrix Protein) Is Structurally Related to the Thrombospondins. *J. Biol. Chem. 267*, 22346–22350.
6. Efimov, V. P., Lustig, A., and Engel, J. (1994) The Thrombospondin-Like Chains of Cartilage Oligomeric Matrix Protein Are Assembled by a 5-Stranded α-Helical Bundle between Residue-20 and Residue-83. *FEBS Lett. 341*, 54–58.
7. Rosenberg, K., Olsson, H., Morgelin, M., and Heinegard, D. (1998) Cartilage oligomeric matrix protein shows high affinity zinc-dependent interaction with triple helical collagen. *J. Biol. Chem. 273*, 20397–20403.
8. Halasz, K., Kassner, A., Morgelin, M., and Heinegard, D. (2007) COMP acts as a catalyst in collagen fibrillogenesis. *J. Biol. Chem. 282*, 31166–31173.
9. Hecht, J. T., Nelson, L. D., Crowder, E., Wang, Y., Elder, F. F. B., Harrison, W. R., Francomano, C. A., Prange, C. K., Lennon, G. G., Deere, M., and Lawler, J. (1995) Mutations in Exon 17b of Cartilage Oligomeric Matrix Protein (Comp) Cause Pseudoachondroplasia. *Nat. Genet. 10*, 325–329.
10. Briggs, M. D., Hoffman, S. M. G., King, L. M., Olsen, A. S., Mohrenweiser, H., Leroy, J. G., Mortier, G. R., Rimoin, D. L., Lachman, R. S., Gaines, E. S., Cekleniak, J. A., Knowlton, R. G., and Cohn, D. H. (1995) Pseudoachondroplasia and Multiple Epiphyseal Dysplasia Due to Mutations in the Cartilage Oligomeric Matrix Protein Gene. *Nat. Genet. 10*, 330–336.
11. Spitznagel, L., Nitsche, D. P., Paulsson, M., Maurer, P., and Zaucke, F. (2004) Characterization of a pseudoachondroplasia-associated mutation (His(587) → Arg) in the C-terminal, collagen-binding domain of cartilage oligomeric matrix protein (COMP). *Biochem. J. 377*, 479–487.
12. Hecht, J. T., Hayes, E., Haynes, R., and Cole, W. G. (2005) COMP mutations, chondrocyte function and cartilage matrix. *Matrix Biol. 23*, 525–533.
13. Kennedy, J., Jackson, G., Ramsden, S., Taylor, J., Newman, W., Wright, M. J., Donnai, D., Elles, R., and Briggs, M. D. (2005) COMP mutation screening as an aid for the clinical diagnosis and counselling of patients with a suspected diagnosis of pseudoachondroplasia or multiple epiphyseal dysplasia. *Eur. J. Hum. Genet. 13*, 547–555.
14. Chen, T. L. L., Posey, K. L., Hecht, J. T., and Vertel, B. M. (2008) COMP mutations: Domain-dependent relationship between abnormal chondrocyte trafficking and clinical PSACH and MED phenotypes. *J. Cell. Biochem. 103*, 778–787.
15. Efimov, V. P., Engel, J., and Malashkevich, V. N. (1996) Crystallization and preliminary crystallographic study of the pentamerizing domain from cartilage oligomeric matrix protein: A five-stranded α-helical bundle. *Proteins: Struct., Funct., Genet. 24*, 259–262.
16. Malashkevich, V. N., Kammerer, R. A., Efimov, V. P., Schulthess, T., and Engel, J. (1996) The crystal structure of a five-stranded coiled coil in COMP: A prototype ion channel? *Science 274*, 761–765.
17. Guo, Y., Bozic, D., Malashkevich, V. N., Kammerer, R. A., Schulthess, T., and Enger, J. (1998) All-trans retinol, vitamin D and other hydrophobic compounds bind in the axial pore of the five-stranded coiled-coil domain of cartilage oligomeric matrix protein. *EMBO J. 17*, 5265–5272.
18. Guo, Y., Kammerer, R. A., and Engel, J. (2000) The unusually stable coiled-coil domain of COMP exhibits cold and heat denaturation in 4−6 M guanidinium chloride. *Biophys. Chem. 85*, 179–186.
19. Ozbek, S., Engel, J., and Stetefeld, J. (2002) Storage function of cartilage oligomeric matrix protein: The crystal structure of the coiled-coil domain in complex with vitamin D-3. *EMBO J. 21*, 5960–5968.
20. Terskikh, A. V., Potekhin, S. A., Melnik, T. N., and Kajava, A. V. (1997) Mutation Gln(54)Leu of the conserved polar residue in the interfacial coiled coil position (d) results in significant stabilization of the original structure of the COMP pentamerization domain. *Lett. Pept. Sci. 4*, 297–304.
21. Slovic, A. M., Summa, C. M., Lear, J. D., and DeGrado, W. F. (2003) Computational design of a water-soluble analog of phospholamban. *Protein Sci. 12*, 337–348.
22. Slovic, A. M., Lear, J. D., and DeGrado, W. F. (2005) De novo design of a pentameric coiled-coil: Decoding the motif for tetramer versus pentamer formation in water-soluble phospholamban. *J. Pept. Res. 65*, 312–321.
23. Liu, J., Yong, W., Deng, Y. Q., Kallenbach, N. R., and Lu, M. (2004) Atomic structure of a tryptophan-zipper pentamer. *Proc. Natl. Acad. Sci. U.S.A. 101*, 16156–16161.
24. Lee, D. L., Mant, C. T., and Hodges, R. S. (2003) A novel method to measure self-association of small amphipathic molecules: temperature profiling in reversed-phase chromatography. *J. Biol. Chem. 278*, 22918–22927.
25. Flaugh, S. L., Mills, I. A., and King, J. (2006) Glutamine deamidation destabilizes human γD-crystallin and lowers the kinetic barrier to unfolding. *J. Biol. Chem. 281*, 30782–30793.
26. Forood, B., Feliciano, E. J., and Nambiar, K. P. (1993) Stabilization of α-helical structures in short peptides via end capping. *Proc. Natl. Acad. Sci. U.S.A. 90*, 838–842.
27. Pace, C. N. (1990) Measuring and Increasing Protein Stability. *Trends Biotechnol. 8*, 93–98.
28. Marky, L. A., and Breslauer, K. J. (1987) Calculating thermodynamic data for transitions of any molecularity from equilibrium melting curves. *Biopolymers 26*, 1601–1620.
29. Beck, K., Gambee, J. E., Bohan, C. A., and Bachinger, H. P. (1996) The C-terminal domain of cartilage matrix protein assembles into a triple-stranded α-helical coiled-coil structure. *J. Mol. Biol. 256*, 909–923.
30. Beck, K., Gambee, J. E., Kamawal, A., and Bachinger, H. P. (1997) A single amino acid can switch the oligomerization state of the α-helical coiled-coil domain of cartilage matrix protein. *EMBO J. 16*, 3767–3777.
31. Johnson, M. L., Correia, J. J., Yphantis, D. A., and Halvorson, H. R. (1981) Analysis of Data from the Analytical Ultra-Centrifuge by Non-Linear Least-Squares Techniques. *Biophys. J. 36*, 575–588.
32. Laue, T. M., Shah, B. D., Ridgeway, T. M., and Pelletier, S. L. (1992) Computer-aided interpretation of analytical sedimentation data for proteins. In Analytical Ultracentrifugation in Biochemistry and Polymer Science (Harding, S. E., Rowe, A. J., and Horton, J. C., Eds.) pp 90−125, Royal Society of Chemistry, Cambridge, U.K.
33. Barik, A., Priyadarsini, K. I., and Mohan, H. (2003) Photophysical studies on binding curcumin to bovine serum albumin. *Photochem. Photobiol. 77*, 597–603.
34. Khopde, S. M., Priyadarsini, K. I., Palit, D. K., and Mukherjee, T. (2000) Effect of solvent on the excited-state photophysical properties of curcumin. *Photochem. Photobiol. 72*, 626–631.
35. Greenfield, N. J. (2006) Using circular dichroism spectra to estimate protein secondary structure. *Nat. Protoc. 1*, 2876–2890.
36. Greenfield, N. J. (2006) Using circular dichroism collected as a function of temperature to determine the thermodynamics of protein unfolding and binding interactions. *Nat. Protoc. 1*, 2527–2535.
37. Pace, C. N., Laurents, D. V., and Thomson, J. A. (1990) pH Dependence of the Urea and Guanidine-Hydrochloride Denaturation of Ribonuclease-a and Ribonuclease-T1. *Biochemistry 29*, 2564–2572.
38. Krylov, D., Barchi, J., and Vinson, C. (1998) Inter-helical interactions in the leucine zipper coiled coil dimer: pH and salt dependence of coupling energy between charged amino acids. *J. Mol. Biol. 279*, 959–972.
39. Walters, M. R. (1992) Newly ientified actions of the vitamin D endocrine system. *Endocrinol. Rev. 13*, 719–764.
40. Bouillon, R., Okamura, W. H., and Norman, A. W. (1995) Structure-function relationships in the vitamin D endocrine system. *Endocrinol. Rev. 16*, 200–257.
41. Means, A. L., and Gudas, L. J. (1995) The roles of retinoids un vertebrate development. *Annu. Rev. Biochem. 64*, 201–233.
42. Marshall, H., Morrison, A., Studer, M., Properl, H., and Krumlauf, R. (1996) Retinoids and Hox genes. *FASEB J. 10*, 969–978.

43. Mehta, K., Pantazis, P., McQueen, T., and Agarwal, B. (1997) Antiproliferative effect of curcumin against human breast tumor cell lines. *Anticancer Drugs 8*, 471–480.
44. Cheng, A. L., Hsu, C. H., Lin, J. K., Hsu, M. M., Ho, Y. F., Shen, T. S., Ko, J. Y., Lin, J. T., Lin, B. R., Wu, M. S., Yu, H. S., Jee, S. H., Chen, G. S., Chen, T. M., Chen, C. A., Lai, M. K., Pu, Y. S., Pan, M. H., Wang, Y. J., Tsai, C. C., and Hsieh, C. Y. (2001) Phase 1 clinical trials of curcumin: A chemopreventive agent in patients with high risk or pre-malignant lesions. *Anticancer Res. 21*, 2895–2900.
45. Barclay, L. R. C., Vinqvist, M. R., Mukai, K., Goto, H., Hasimoto, Y., Tokunaga, A., and Uno, H. (2000) On the antioxidant mechanism of curucmin: Classical methods are needed to determine antioxidant mechanism and activity. *Org. Lett. 2*, 2841–2843.
46. Balasubramanyam, K., Varier, R. A., Altaf, M., Swaminathan, V., Siddappa, N. B., Ranga, U., and Kundu, T. K. (2004) Curcumin, a novel p300/CREB-binding protein-specific inhibitor of acetyltransferase, represses the acetylation of histone/nonhistone proteins and histone acetyltransferase-dependent chromatin transcription. *J. Biol. Chem. 279*, 51163–51171.
47. Morimoto, T., Sunagawa, Y., Kawamura, T., Takaya, T., Wada, H., Nagasawa, A., Komeda, M., Fujita, M., Shimatsu, A., Kita, T., and Hasegawa, K. (2008) The dietary compound curcumin inhibits p300 histone acetyltransferase activity and prevents heart failure in rats. *J. Clin. Invest. 118*, 868–878.
48. Mason, J. M., and Arndt, K. M. (2004) Coiled coil domains: Stability, specificity, and biological implications. *ChemBioChem 5*, 170–176.
49. Landschulz, W. H., Johnson, P. F., and McKnight, S. L. (1988) The Leucine Zipper: A Hypothetical Structure Common to a New Class of DNA-Binding Proteins. *Science 240*, 1759–1764.
50. Gunasekar, S. K., Haghpanah, J. S., and Montclare, J. K. (2008) Assembly of bioinspired helical protein fibers. *Polym. Adv. Technol. 19*, 454–468.
51. Harbury, P. B., Zhang, T., Kim, P. S., and Alber, T. (1993) A Switch between 2-Stranded, 3-Stranded and 4-Stranded Coiled Coils in Gcn4 Leucine-Zipper Mutants. *Science 262*, 1401–1407.
52. Montclare, J. K., Sloan, L. S., and Schepartz, A. (2001) Electrostatic control of half-site spacing preferences by the cyclic AMP response element-binding protein CREB. *Nucleic Acids Res. 29*, 3311–3319.
53. Diss, M. L., and Kennan, A. J. (2008) Orthogonal recognition in dimeric coiled coils via buried polar-group modulation. *J. Am. Chem. Soc. 130*, 1321–1327.
54. Deng, Y. Q., Liu, J., Zheng, Q., Li, Q. N., Kallenbach, N. R., and Lu, M. (2008) A Heterospecific Leucine Zipper Tetramer. *Chem. Biol. 15*, 908–919.
55. Takei, T., Okonogi, A., Tateno, K., Kimura, A., Kojima, S., Yazaki, K., and Miura, K. (2006) The effects of the side chains of hydrophobic aliphatic amino acid residues in an amphipathic polypeptide on the formation of a helix and its association. *J. Biochem. 139*, 271–278.
56. Simmerman, H. K. B., Kobayashi, Y. M., Autry, J. M., and Jones, L. R. (1996) A leucine zipper stabilizes the pentameric membrane domain of phospholamban and forms a coiled-coil pore structure. *J. Biol. Chem. 271*, 5941–5946.
57. Slovic, A. M., Stayrook, S. E., North, B., and DeGrado, W. F. (2005) X-ray structure of a water-soluble analog of the membrane protein phospholamban: Sequence determinants defining the topology of tetrameric and pentameric coiled coils. *J. Mol. Biol. 348*, 777–787.
58. Liu, J., Zheng, Q., Deng, Y. Q., Cheng, C. S., Kallenbach, N. R., and Lu, M. (2006) A seven-helix coiled coil. *Proc. Natl. Acad. Sci. U.S.A. 103*, 15457–15462.
59. Shen, W., Zhang, K. C., Kornfield, J. A., and Tirrell, D. A. (2006) Tuning the erosion rate of artificial protein hydrogels through control of network topology. *Nat. Mater. 5*, 153–158.
60. Papapostolou, D., Smith, A. M., Atkins, E. D. T., Oliver, S. J., Ryadnov, M. G., Serpell, L. C., and Woolfson, D. N. (2007) Engineering nanoscale order into a designed protein fiber. *Proc. Natl. Acad. Sci. U.S.A. 104*, 10853–10858.
61. Woolfson, D. N., and Ryadnov, M. G. (2006) Peptide-based fibrous biomaterials: Some things old, new and borrowed. *Curr. Opin. Chem. Biol. 10*, 559–567.
62. Woolfson, D., Pandya, M., Ryadnov, M., and Smith, A. (2005) Designing nano-to-micron scale peptide-based self-assembling systems from the bottom up. *Biopolymers 80*, 493–493.
63. Fairman, R., and Ankerfedt, K. S. (2005) Peptides as novel smart materials. *Curr. Opin. Struct. Biol. 15*, 453–463.